

AMD - Vol. 43



1981 Biomechanics Symposium



1981 Biomechanics Symposium

presented at the

JOINT ASME/ASCE MECHANICS CONFERENCE
UNIVERSITY OF COLORADO
BOULDER, COLORADO
JUNE 22-24, 1981

edited by

WILLIAM C. VAN BUSKIRK
TULANE UNIVERSITY

SAVIO L-Y. WOO
UNIVERSITY OF CALIFORNIA AT SAN DIEGO

THE AMERICAN SOCIETY OF MECHANICAL ENGINEERS
United Engineering Center 345 East 47th Street New York, N. Y. 10017

FOREWORD

The 1981 ASME Biomechanics Symposium is the fifth consecutive symposia offered on a biyearly basis (in the odd-numbered years). The first symposium was organized by Professors Y. C. Fung and J. A. Brighton under the joint-sponsorship of the Applied Mechanics and Fluids Engineering Divisions. The purpose has been to provide a continuing forum which is devoted principally to the mechanics aspect of bioengineering.

As a result of the 1973 symposium, the Joint Biomechanics Committee, under the auspices of the Applied Mechanics Division, the Fluids Engineering Division, and later, the Bioengineering Division, was formed. The primary goal of this committee has been to unify and to coordinate biomechanics activities among the divisions in ASME and other sister societies, and to organize this biyearly symposium. This 1981 Biomechanics Symposium also has the pleasure, for the first time, of the Joint sponsorship of our sister society, ASCE, and its Bioengineering Committee, headed by Professors T. K. Hung and G. C. Lee.

During the past eight years we have witnessed the blossoming of biomechanics activities in terms of the attendance, the number of abstracts submitted, and the program of the symposia. This year the Biomechanics Committee had a particularly difficult task in selecting papers for the symposium. There were 95 abstracts submitted (a record), and there were only 64 slots allowed for paper presentation. As a result, the program committee found it necessary to add a new category in which 14 additional papers that the referees considered to be of sufficiently high quality are included in the Symposium Proceedings, but without presentation. The 64 accepted papers for presentation are divided into eight sessions with three sessions devoted to biofluid mechanics, and five to biosolid mechanics.

The 1981 Biomechanics Symposium is particularly exciting because there is a parallel symposium on "Mechanical Properties of Bone" organized by Professor S. C. Cowin. We have planned a joint session to start out both of the Symposia. In addition, the 1981 Biomechanics Symposium includes several presentations which are contributions from foreign countries, and finally, we have the honor of having Professor Richard Skalak give one of the keynote lectures as part of this ASME/ASCE Mechanics Conference. His title is "Biomechanics: Past, Present and Future."

Savio L-Y. Woo
William C. Van Buskirk

ACKNOWLEDGMENTS

We wish to recognize the members of the Organizing Committee —

ASME Joint Biomechanics Committee —

D. L. Butler	University of Cincinnati, Secretary
C. Brennan	California Institute of Technology
A. H. Burstein	Hospital for Special Surgery
R. E. Mates	State University of New York at Buffalo
V. C. Mow	Rensselaer Polytechnic Institute
T. Mueller	University of Notre Dame
R. M. Nerem	University of Houston (Past Chairman)
A. B. Schultz	University of Illinois at Chicago Circle (Past Chairman)
R. Skalak	Columbia University (Past Chairman)
C. R. Steele	Stanford University
D. D. Streeter, Jr.	Children's Orthopedic Hospital and Medical Center, Seattle
M. Wells	Colorado State University
W. J. Yang	University of Michigan

ASCE Bioengineering Committee —

T. K. Hung	University of Pittsburgh, Chairman
G. C. Lee	State University of New York at Buffalo
S. C. Anand	Clemson University
T. Belytschko	Northwestern University
H. Chen	Georgia Institute of Technology
M. E. Clark	University of Illinois
M. Lai	Rensselaer Polytechnic Institute
L. McIntyre	Rice University
V. C. Mow	Rensselaer Polytechnic Institute
L. F. Mocos	Northwestern University
H. Scarton	Rensselaer Polytechnic Institute
R. Skalak	Columbia University

We would like to thank the following reviewers who refereed the abstracts for the 1981 Biomechanics Symposium program:

K. N. An	J. L. Lewis
T. P. Andriacchi	Y. K. Liu
G. C. Armstrong	L. McIntyre
D. L. Bartel	G. Mansour
T. Belytschoko	R. E. Mates
T. D. Brown	L. F. Mockros
D. L. Butler	V. C. Mow
A. H. Burstein	T. M. Mueller
D. Carter	R. M. Nerem
Y. S. Chao	M. Panjabi
C. J. Chen	Y. C. Pao
H. Chen	J. Pinto
M. E. Clark	R. Piziali
F. R. Convery	V. Roth
S. C. Cowin	H. Scarton
R. D. Crowninshield	G. Schmid-Schoenbein
Y. C. Fung	A. B. Schultz
D. N. Ghista	A. Seireg
E. S. Grood	R. Skalak
S. Hampton	C. R. Steele
R. C. Haut	D. D. Streeter, Jr.
W. C. Hayes	P. Torzilli
V. M. Lai	M. Wells
L. Latta	Y. T. Yen

Savio L-Y. Woo
William C. Van Buskirk
Co-Chairmen, Joint Biomechanics Committee

CONTENTS

Correlation of in vitro Fluid Dynamics of Prosthetic Heart Valves with in vivo Performance <i>A. P. Yoganathan and E. C. Harrison</i>	1
Backflow Considerations in the Design of Prosthetic Heart Valves <i>K. C. Dellsperger and D. W. Wieting</i>	3
The in vitro Fluid Dynamics of the Hall-Kaster and New Bjork-Shiley Heart Valve Prostheses <i>D. M. Stevenson, A. P. Yoganathan and R. H. Franch</i>	7
The Effects of Tissue Anisotropy on the Mechanics of Bioprosthetic Heart Valves <i>G. W. Christie and I. C. Medland</i>	11
Three Dimensional Finite Element Reconstruction of Left Ventricular Geometry from Cross-Sectional Echo Cardiographic Recordings <i>P. E. Nikravesh, K. B. Chandran, D. J. Skorton, N. Pandian and R. E. Kerber</i>	15
Deformation and Stress Analysis of the Left Ventricle: An Active Thick Ellipsoidal Model <i>C-J Chen, M-C Hsu, K. Rim and H. L. Falsetti</i>	19
The Relative Contribution of the Subendocardium and Subepicardium to Systolic Left Ventricular Wall Thickness <i>H. N. Sabbah, M. Marzilli and P. D. Stein</i>	23
Quantification of Regional Heart Muscle Contraction in Intact Thorax <i>Y. C. Pao, P. A. Chevalier and E. L. Ritman</i>	27
In Vitro Measurements of Turbulence in the Vicinity of a Prosthetic Heart Valve <i>R. S. Figliola and T. J. Mueller</i>	31
Microprocessor Controlled Multigate Pulsed Ultrasound Doppler Technique for Quantitative Velocity and Flow Measurement <i>M. Casty, D. P. Giddens and M. Anliker</i>	35
Multiplexed Doppler Flowmetry <i>M. B. Histand, M. K. Wells and R. Corace</i>	39
Vascular Endothelial Morphology as an Indicator of the Pattern of Blood Flow <i>R. M. Nerem, M. J. Levesque and J. F. Cornhill</i>	43
Velocity Measurements of Pulsatile Flow Through a Cast of an Asymmetric Human Aortic Bifurcation <i>F. F. Mark, C. B. Barger, O. J. Deters, G. M. Hutchins and M. H. Friedman</i>	47
Flow Resonance in Curved Artery Models <i>J. M. Tarbell, S. Kang and J. Y. Lin</i>	51
A Computation of Three-Dimensional Flows in Deformable Curved Tubes <i>T-K Hung and W-S Cheng</i>	55
Unsteady Flow in Collapsible Tubes <i>R. Collins and A. Tedgui</i>	57
Phenomenological Laws for Platelet Transport <i>E. C. Eckstein</i>	61
Cavitation Effects Near Moving Prosthetic Surfaces <i>W. F. Walker and C. M. Dube</i>	65
Transport in Rotating Tubular Oxygenators <i>J. Berman and L. F. Mockros</i>	69

New Instrumentation for Density Profiles in Microscopic Tube Flow <i>A. B. Corbet, B. Strul, C. Holliger, G. S. Harrell.</i>	73
A High Deformation Rate Estimate of Erythrocyte Membrane Viscosity by Flow Through Pores <i>E. A. O'Rear and L. V. McIntire.</i>	75
Red Cell Shapes in Micropipettes <i>B. K. Pai</i>	77
Measurements of the Red Cell Membrane Shear Modulus Using an Extensional Hyperbolic Flow <i>L. M. Trebing, S. P. Suter and R. A. Gardner.</i>	81
The Prediction of Force in Normal Muscle Function <i>R. D. Crowninshield and R. A. Brand</i>	85
Particle Charge Effect of Deposition of Therapeutic Aerosols in the Tracheo-bronchial Tree During Inspiration <i>C. P. Yu.</i>	89
A Constitutive Model for Passive Skeletal Muscle Based on Anatomic Considerations <i>D. L. Bugler and R. W. Little.</i>	93
A Model for Quantifying Static Load, Incorporating Muscle Fatigue <i>J. M. M. Huijgens.</i>	97
Determination of the Coefficients in the Equilibrium Equations for Muscles <i>K. N. An, T. P. Harrigan, B. P. Cahill and E. Y. S. Chao</i>	101
On Optimality in Structural and Material Composition of Bamboo <i>J. Oda.</i>	105
Performance Analysis of Bicycle Pedalling <i>R. R. Davis and M. L. Hull</i>	109
Torque Generation on Wheelchair Handrims <i>R. L. Brauer and B. A. Hertig.</i>	113
Reflex Feedback in Small Perturbations of a Limb <i>S. C. Cannon and G. I. Zahalak</i>	117
The Mechanical Design of a Cranial Probe Guide <i>R. Lipp, B. Bishop, R. McAfee and M. Correa.</i>	121
Three-Dimensional Stress Distribution in Arteries Under the Assumptions of In-Compressibility and Homogeneity <i>C. J. Choung and Y. C. Fung</i>	125
The Axial Force and Torque Response of the Anterior Cruciate Ligament of a Dog <i>D. Stouffer, D. L. Butler.</i>	129
Unconfined Compression of Articular Cartilage <i>C. G. Armstrong, W. M. Lai and V. C. Mow</i>	133
Variation of the Intrinsic Aggregate Modulus and Permeability of Articular Cartilage with Trypsin Digestion <i>T. M. Stahurski, C. G. Armstrong and V. C. Mow.</i>	137
The Effects of Leucocytic Elastase on the Tensile Properties of Adult Human Articular Cartilage <i>G. E. Kempson</i>	141
A Viscoelastic Model of the Shear Response of the Intervertebral Disc <i>B. S. Kelley, J. F. Lafferty, D. A. Bowman and P. A. Clark</i>	145
Elastic Properties of the Dog Trachea In-Vivo <i>D. C. Winter, R. L. Pimmel and B. F. Lewis</i>	149

Biomechanical Behavior of Fetal Dura Mater <i>T. J. Kriewall, N. Akkas, D. Bylski, J. W. Melvin and B. A. Work, Jr.</i>	153
The Elastic Modulus of Fetal Skull Bone <i>T. J. Kriewall, J. W. Melvin and B. A. Work, Jr.</i>	155
Relative Importance of Skull Deformation <i>M. Chan, C. Ward, D. Schneider and S. Adams</i>	157
Feedback Mechanisms of Bones Due to Various Stimuli <i>N. Guzelsu</i>	161
Effect of Couple Stresses in Compact Bone: Dynamic Experiments <i>R. S. Lakes</i>	165
Permeability of Compact Bone <i>S. W. Rouhana, M. W. Johnson, D. A. Chakkalakal, R. A. Harper and J. L. Katz</i>	169
Model Analysis of Human Tibia <i>G. Van der Perre, R. Van Audekercke, J. Van de Castele, M. Martens and J. C. Mulier</i>	173
Generalized Resonances of the Isolated Femur <i>T. B. Khalik, D. C. Viano</i>	177
Tensile Strains Associated with Compression of the Femur <i>D. C. Viano and T. B. Khalil</i>	181
Guidelines for Optimal Experimental Design to Study Joint Kinematics Using Instant Axis Concept <i>M. M. Panjabi, S. Walters and V. K. Goel</i>	185
Standards for Mechanical Knee Analysis of (Sideways) Bending <i>J. T. Bryant</i>	189
The Computerized Knee Analyses <i>D. Siu and H. W. Weavers</i>	193
The Development of a Mathematical Model of the Knee Joint Used to Investigate Passive Medio-Lateral Stability <i>G. J. Gouw and H. W. Weavers</i>	197
Contact Stress Distribution Measurements in the Human Hip Joint <i>T. D. Brown and D. T. Shaw</i>	201
Tabecular Morphology and Biomechanics of the Human Pelvis <i>H. J. Rubenstein, M. T. Manley, M. Badalamente and L. Stern</i>	205
Facet Loading in Lumbar Motion Ligaments <i>J. A. A. Miller, K. A. Haderspeck and A. B. Schultz</i>	209
An Analysis of Normal Wrist Kinematics <i>R. B. Brumbaugh and R. D. Crowninshield</i>	213
An Investigation of the Method of Degradation of Flexible Carbon Fibers Used for Ligament and Tendon Repair <i>N. R. Miller and G. J. Pijanowski</i>	217
Analytic Guidelines for Optimal Stem Designs of Custom-Made Joint Prostheses <i>R. Huiskes, T. E. Crippen, J. E. Bechtold and E. Y. Chao</i>	221
Measurement of Joint Forces with Implants, A New Method of Instrumentation and Its Application in Sheep <i>G. Bergmann, J. Siraky, R. Kolbel and A. Rohlmann</i>	225
A Technique for Analytical Representation of Normative Articular Surfaces <i>H. J. Sommer III and N. R. Miller</i>	229

Contact Area Pressure Distribution in Contemporary Total Knee Designs <i>R. W. Hood, T. M. Wright, T. Fukubayashi and A. H. Burstein</i>	233
Acoustic Emission Monitoring in the Diagnosis of Loosening in Total Knee Arthroplasty <i>T. M. Wright, R. W. Hood, and W. J. Flynn.</i>	237
Biomechanical Analysis of Scoliosis Correctional Devices: Specifications for the Corrective Forces in Terms of the Achievable Corrections <i>D. N. Ghista, G. Jayaraman, R. Romick, and R. Jacobs.</i>	241
Axisymmetric Analysis of Pin-Bone Interface Stresses of External Fixation Devices <i>T. E. Crippen, R. Husikes and E. Y. Chao.</i>	247
Left Ventricular Noninvasive Diagnostic Patterns Derivable From Cycle Ventricular Blood Inflow-Outflow Rate Dynamics, Cyclic Myocardial Wall Kinematics and First Heart Sound Spectral Frequency <i>D. N. Ghista and T. Moskal</i>	251
The Force-Attenuating Properties of the Musculoskeletal System as a Function of Body Weight <i>A. Voloshin, J. Wosk</i>	255
Measuring the Force Distribution Under the Foot as a Means of Evaluating Running Shoes <i>A. H. Hoffman, K. R. Fast, C. M. Ingalls and H. T. Grandin, Jr.</i>	259
Analysis of Quadriceps Loading in Bicycling <i>M. L. Hull and R. Butler.</i>	263
Wheelchair Rolling Resistance <i>R. L. Brauer, and P. J. Voegtle.</i>	267
Structural Composite Model for Large Deformations of the Anterior Cruciate Ligament <i>P. S. Thirty, M. A. Tabbal, G. Drouin, and C. A. Laurin</i>	271
Interdigitation of Methylmethacrylate and Cancellous Bone vs. Medullary Injection Pressure <i>M. M. Panjabi, H. Drinker, V. K. Goel, G. C. Kammire and J. Wong.</i>	275
Anisotropic Nature of the Ultrasonic Characteristics of Cancellous Bone <i>S. Saha, S. Pal, V. Rao</i>	279
In Vivo Torsional Evaluation of Spinal Orthoses <i>J. F. Passerman, M. J. McNamee.</i>	283
The Mechanical Properties of Pseudarthrosis in Posterior Spinal Fusion in Canine Models: A Preliminary Report <i>R. Vanderby Jr., C. A. Sciammarella, S. S. Lei, T. Stoncipher, and J. Fisk . .</i>	287
A Technique for Mechanical Assessment of the Intervertebral Joint <i>M. Lubin, M. Brown and E. C. Eckstein.</i>	291
Loads Transmitted by Lower Limb Orthoses <i>N. Berne, A. E. Trappitt</i>	295
Development of the Rat Acetabulum: A Contribution to the Understanding of Congenital Hip Dislocation <i>E. E. Sabelman</i>	299
A Simple Device to Measure Range of Joint Motion <i>L. E. Carlson</i>	303
List of Related Titles	307

CORRELATION OF IN VITRO FLUID DYNAMICS
OF PROSTHETIC HEART VALVES WITH IN VIVO PERFORMANCE

by

Ajit P. Yoganathan* and Earl C. Harrison⁺

*School of Chemical Engineering
Georgia Institute of Technology
Atlanta, Georgia 30332

⁺Cardiology Section, USC-LA County Medical Center
Los Angeles, California 90033

Some of our clinical and pathologic observations, and in vitro fluid dynamic experiences with the Bjork-Shiley, Starr-Edwards (ball valves), Smeloff-Cutter and Kay-Shiley prosthetic valves are discussed. It is quite clear that at present there is no ideal prosthetic heart valve. The major problems that affect the mechanical valves are thromboembolism and tissue overgrowth. The observed problems of thrombus formation, tissue overgrowth, red cell destruction and damage to the endothelial lining of the vessel walls adjacent to the valve prostheses are directly related to the hemodynamics of the respective prostheses. It is our experience that all mechanical prosthetic heart valves that are presently commercially available are liable to thrombus formation and tissue overgrowth. Therefore, correlative studies such as described in this article should be conducted with all heart valve prostheses. Detailed pathologic studies on approximately 150 to 200 recovered prosthetic heart valves of different types are presently in progress.

In our clinical use of the Bjork-Shiley aortic prosthesis we have observed thrombus formation and tissue overgrowth in ten aortic prostheses recovered six months or longer after implantation. Such thrombus formation and tissue overgrowth have also been observed by others. These pathologic findings may be attributed to the flow characteristics of the prosthesis. The open disc of the valve separates the flow into two unequal regions. Varying degrees of the thrombus formation were observed in the minor outflow region, including the depression in the aortic face of the disc and the metal strut bridging this area. Tissue overgrowth was noted along the perimeter of the prosthesis adjacent to the minor outflow region. That overgrowth further reduced the available cross section for flow in this already constrained area. In vitro measurements with a laser-Doppler anemometer identified a zone of stagnation about 20 mm wide near the aortic face of the disc of a size #27 Bjork-Shiley valve. The average velocities in the major and minor outflow regions were around 100 and 25 cm/s, respectively, and the corresponding peak shear stresses were approximately 70 and 15 N/m². There is reason, then, to attribute the thrombus formation and tissue overgrowth to the stagnation zone and the low shear in the minor outflow region.

Examinations were made at the USC-Los Angeles County Medical Center of 15 Starr-Edwards aortic ball valve prostheses recovered during autopsy and/or surgery. Thrombus formation and tissue overgrowth were observed at various locations on the recovered valves. Varying amounts of thrombus formation were observed predominantly at the base of the struts and the apex of the cage, while varying degrees of tissue overgrowth were predominantly observed on the aortic side of the sewing ring and on the struts of the cloth covered valves. In some cases the thrombus had grown along the struts, probably starting either at the apex or the base of the struts. In addition, examination of the vessel walls immediately downstream of the valve sewing rings indicated varying degrees of endothelial damage and fibrous tissue proliferation in some of the specimens. Detailed pathologic studies on the recovered valves are in progress at the present time.

Our *in vitro* studies on a 1260-12A valve (sewing ring: 27 mm), indicate that the Starr-Edwards ball valves have major fluid dynamic drawbacks such as: (a) relatively large pressure drops, (b) hydrodynamically unstable poppet, (c) regions of flow separation at the base of each of the three struts, (d) region of flow stagnation at the apex of the cage (~ 7 to 15 mm in diameter), (e) large wall-shear stresses (~ 50 -200 N/m² and bulk turbulent shear stresses (on the order of 10-500 N/m² in the immediate downstream vicinity of the valve, and (f) large shear stresses adjacent to the poppet surface and struts (on the order of 10-10³ N/m²).

The observed stagnation zone could encourage thrombus formation on the apex of the cage, while the observed regions of flow separation could lead to thrombus formation and tissue overgrowth at the base and upwards along the struts. The observed wall shear could lead to damage of endothelial tissue in the proximal ascending aorta, to hemolysis, and to thrombus formation. In addition, the elevated shears adjacent to the struts and the surface of the poppet could lead to increased hemolysis with those Starr-Edwards ball valves having cloth covered struts.

Our clinical experience with the Smeloff-Cutter valve has been very satisfactory. Of a total of 46 patients followed over a period of 8 years, two patients had pulmonary embolism and only one had a case of bland systemic embolism. Fifteen of sixteen patients had mild hemolysis as evidenced by increased serum lactic dehydrogenase or decreased haptoglobin or presence of urinary hemosiderin. No ball variance or other types of material failure were detected in eight valves that were recovered at autopsy. Most of the recovered Smeloff-Cutter aortic valves showed no regions of thrombus formation and/or tissue overgrowth on the valve superstructure. A few (2 or 3) of the recovered valves showed small amounts of thrombus formation at the base of the aortic side of the struts. Examination of the vessel walls immediately downstream of the valve sewing rings indicated varying degrees of endothelial damage and fibrous tissue proliferation in some of the specimens.

Our *in vitro* flow studies on a A5 Smeloff-Cutter valve (sewing ring: 26 mm) indicated that this peripheral flow valve creates relatively high wall shear stresses (~ 167 N/m²). The velocities near the apex of the cage were negative and on the order of -10 to -20 cm/s. This may produce a mild "washing" effect and tend to prevent material adhering to the apex of the cage. A region of flow separation was observed near the base of the aortic side of the struts. Such a region of flow separation could lead to thrombus formation at the base of the aortic side of the struts. Bulk turbulent shear stresses on the order of 100 to 400 N/m² were observed in the immediate downstream vicinity of the valve. Such turbulent shear stresses could cause lethal and/or sub-lethal damage to blood components.

Our clinical experience with this valve stems from the study of 82 Kay-Shiley mitral valve recipients. Of a group of 63 patients followed in the clinic the incidence of arterial thromboembolism occurred in seven of the 63 patients. Of the 20-Kay-Shiley valves examined at autopsy, eleven had thrombus formation and/or tissue overgrowth on the valve superstructure. The thrombus formation mainly occurred at the base of the valve struts. Tissue overgrowth occurred along the ventricular side of the sewing ring. The thrombus formation and tissue overgrowth in some instances prevented the disc from seating properly and thereby causing the valve to leak during ventricular systole. The thrombus formation and/or tissue overgrowth could be attributed to the regions of flow separation observed at the base of the struts. Another problem observed with this valve was the grooving and notching of the Delrin disc. The grooving and notching of the disc was due to the prevention of proper disc motion because of thrombus and/or tissue overgrowth on the superstructure. Proper disc motion includes movement up and down the cage during the cardiac cycle as well as rotation.

BACKFLOW CONSIDERATIONS IN THE DESIGN OF PROSTHETIC HEART VALVES

Kevin C. Dellsperger, B.S.
Department of Physiology and Biophysics
LSU Medical Center
Shreveport, LA 71130
and
David W. Wieting, Ph.D.
Mitral Medical International, Inc.
Irvine, CA 92714

INTRODUCTION

A major consideration in the selection of a prosthetic heart valve is the amount of backflow associated with a particular design⁽¹⁾. For the patient with poor cardiac performance, the amount of backflow may become critical, particularly when cardiopulmonary bypass is terminated and low cardiac output persists due to decreased heart rate and low stroke volume.

Backflow associated with prosthetic heart valves is composed of two different types: I. Closure (which is required to close the valve), and II. Leakage (which occurs after the valve is closed). See Fig. 1.

Although studies of backflow associated with prosthetic heart valves have been reported with varying conditions a detailed analysis of backflow associated with heart valves under varying heart rates and cardiac outputs has not been conducted⁽²⁾.

METHODS

Two currently available size 27 mm prosthetic aortic valves (a Bjork-Shiley and an Ionescu-Shiley Pericardial Xenograft) were studied in the aortic chamber of a pulse duplication system which models the left heart as described by Wieting in 1969⁽³⁾. The Bjork-Shiley valve was tested using an aqueous glycerol blood analog fluid composed of 36.7% glycerol by volume. The specific gravity of this solution at 25°C is 1.1 with a viscosity of 3.5cP. The Ionescu-Shiley valve was tested using normal saline.

The pulse duplication system was "tuned" by monitoring left atrial, left ventricular, and aortic pressures. These pressures were measured by means of three Ailtech MS20 Physiologic Pressure Transducers. Aortic flow was measured with a Carolina Square-Wave Electromagnetic Flowmeter, Model 501, using a 26 mm diameter cannulating probe. The pressure and flow were signals were monitored and recorded on an Electronics for Medicine VR-6 Simultrace Recorder using paper speeds of 100 mm/sec.

Heart rates, cardiac outputs, and systolic durations, corresponding to the QT interval on the electrocardiogram⁽⁴⁾, used were:

<u>Heart Rate</u> (bpm)	<u>Cardiac Outputs</u> (lpm)	<u>Systolic Duration</u> (msec)
50	2,4	420
80	2,4,6	350
110	2,4,6,8	290
140	2,4,6,8	260

Throughout the range of simulated heart rates and cardiac outputs the mean aortic pressure was maintained at 100 ± 2 mm Hg, and mean left atrial pressure was maintained at physiologic levels, not exceeding 18 mm Hg at the rapid "heart rate" and high "cardiac output" settings.

RESULTS AND DISCUSSION

Backflow results were analyzed by planimetry techniques in two major categories, 1. the percent backflow and 2. backflow measured in cc/stroke. The two major categories were further divided into closure, leakage and total backflow (see Figure 1). Backflow in cc/stroke is obtained from the formula⁽¹⁾:

$$\text{Backflow (cc/stroke)} = \frac{A_n}{(A_1 - A_2)} \times \frac{CO}{HR}, \quad (n = 2, 3, 4)$$

where: A_1 is the area of the forward flow is the curve
 A_2 is the area of total backflow
 A_3 is the area of backflow during valve closure
 A_4 is the area of backflow during valve leakage
 CO is the mean flow rate in ml/min
 HR is the pulse rate in beats/min

The results are shown in Tables 1 and 2. The Ionescu-Shiley Pericardial Xenograft as a tissue-type valve has only closure backflow since once the valve is closed leakage does not occur. However, the Bjork-Shiley has both closure and leakage types of backflow. The percent total backflow for the Bjork-Shiley range from 8.9% (at 110 beats/min and 8 liters/min) to 36.0% (at 140 beats/min and 2 liters/min). The Ionescu-Shiley on the other hand has total percent backflow that ranges from 5.7% (at 50 beats/min and 4 liters/min) to 21.2% (at 140 beats/min and 2 liters/min).

Of particular interest regarding the Ionescu-Shiley Pericardial Xenograft is that backflow in cc/stroke remains relatively constant throughout the ranges studied with a mean of 4.5 ± 0.1 (\pm SEM) cc/stroke and a range of 3.8 to 4.8 cc/stroke. Since this type of valve does not possess leakage type backflow, the total backflow is equivalent to the closure-type of backflow. The backflow results for the Bjork-Shiley in cc/stroke are as follows: total backflow = 9.4 ± 1.0 cc/stroke (mean \pm SEM), closure backflow = 5.1 ± 0.2 cc/stroke; and leakage backflow = 4.3 ± 0.9 cc/stroke. As seen with the Ionescu-Shiley valve, the closure-type backflow of the Bjork-Shiley valve did not vary significantly with the various settings of the pulse duplication system having a range of 3.5 to 6.0 cc/stroke. However, the leakage-type backflow measured in cc/stroke varies with heart rate through an inverse linear relationship. This relationship is due to the decreased time for leakage to occur as heart rate increases, and diastole concurrently decreases. Wright⁽²⁾ in 1977 reported similar findings in a study mitral valves at a constant stroke volume and varying heart rates.

CONCLUSION

Prosthetic heart valves should be designed to minimize closure backflow; however, it is equally as important to design valves with minimal leakage backflow since at low heart rates, leakage is the predominant factor.

REFERENCES

1. Dellsperger, K.C., D.W. Wieting, D.A. Baehr, R.J. Bard, J.P. Brugger and E. C. Harrison. "Regurgitation of Prosthetic Heart Valves: Dependence on Heart Rate and Cardiac Output." In Press.
2. Wright, J.T.M. "An in-vitro assessment of the Hydraulic Characteristics of the Mark II Abrams-Lucas Mitral Valve Prosthesis." *Thorax*, 32:296-302. 1977.
3. Wieting, D.W. Dynamic Flow Characteristics of Heart Valves. Ph.D. Dissertation. University of Texas, Austin, Texas. May 1969.
4. Burton, A.C. Physiology and Biophysics of the Circulation. Yearbook Medical Publishers, Chicago, IL. 1965, p. 123.

Table 1. Backflow Results in cc/stroke.

Bjork-Shiley					Ionescu-Shiley					
Heart Rate (beats/min)					Heart Rate (beats/min)				cc/stroke	
					50	80	110	140		
Cardiac Output (Liters/min)	2	50	80	110	140	50	80	110	140	
		5.5	6.0	5.2	6.0	4.3	4.4	4.6	3.8	closure
		11.8	6.8	3.6	1.9	NM	NM	NM	NM	leakage
		17.3	12.8	8.8	7.9	4.3	4.4	4.6	3.8	total
	4	5.3	5.0	5.0	5.4	4.8	4.7	4.8	4.1	closure
		10.0	5.6	3.7	2.0	NM	NM	NM	NM	leakage
		15.3	10.6	8.7	7.4	4.8	4.7	4.8	4.1	total
	6	X	4.6	5.1	4.6	X	4.8	4.6	4.2	closure
			4.1	1.6	1.2		NM	NM	NM	leakage
			8.7	6.7	5.8		4.8	4.6	4.2	total
	8	X	X	5.0	3.5	X	X	4.6	4.2	closure
				2.1	2.1			NM	NM	leakage
7.1				5.6	4.6			4.2	total	
Means at constant HR	5.4	5.2	5.1	4.9	4.6	4.6	4.6	4.1	closure	
	10.9	5.5	2.7	1.8	NM	NM	NM	NM	leakage	
	16.3	10.7	7.8	6.7	4.6	4.6	4.6	4.1	total	

*- Not Measurable

Table 2. Backflow Results in Percent Total Backflow.

		Bjork-Shiley				Ionescu-Shiley			
		Heart Rate (beats/min)				Heart Rate (beats/min)			
		50	80	110	140	50	80	110	140
Cardiac Output (liters/min)	2	30.3	33.4	32.6	36.0	9.8	15.1	20.1	21.2
	4	16.0	17.6	19.2	20.6	5.7	8.7	11.7	12.5
	6	X	10.4	11.0	11.9	X	6.0	7.8	8.9
	8	X	X	8.9	8.9	X	X	5.9	6.8

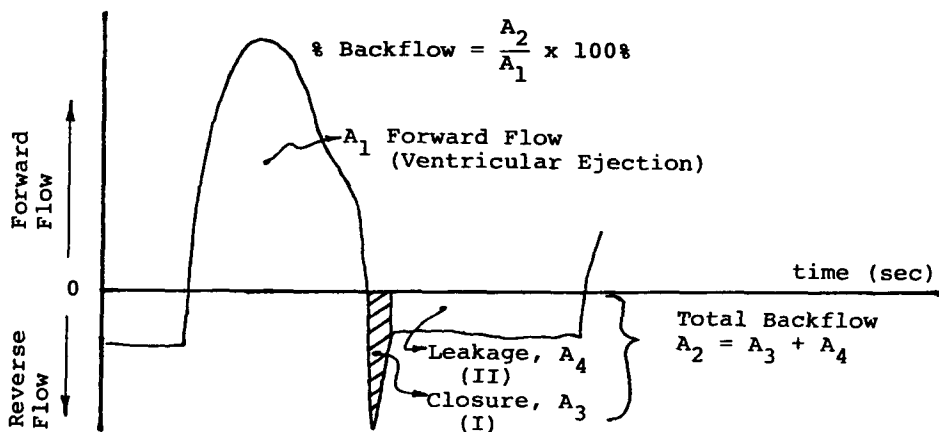


Figure 1. Typical aortic flow versus time tracing illustrating categories of backflow.

THE IN VITRO FLUID DYNAMICS OF THE
HALL-KASTER AND NEW BJORK-SHILEY
HEART VALVE PROSTHESES

by

Dana M. Stevenson, Ajit P. Yoganathan and Robert H. Franch*
School of Chemical Engineering, Georgia Tech
Atlanta, Georgia 30332

*Cardiology Laboratory, Emory University Hospital
Atlanta, Georgia 30322

With the current speculations about the durability of tissue valve prostheses, manufacturers are designing new types of mechanical valves such as the St. Jude, Hall-Kaster and Omni-Science, and modifying existing designs to improve their hemodynamic (fluid dynamic) performance. In the present paper we will discuss the fluid dynamic characteristics of one of the newer valve designs (Hall-Kaster), and a modified version (1980) of the most popular mechanical valve (Bjork-Shiley) in current clinical use. Both designs are known as tilting disc type valves.

The Hall-Kaster valve is composed of a flat circular disc of pyrolytic carbon within a titanium housing. The housing is machined from a single-solid piece of titanium, eliminating the need for welds. The disc pivots at an angle of 75° in the aortic design, and 70° in the mitral design, in the fully open position. The disc is marked by a radio-opaque marker. In addition, a minor modification has been made to the metal stops and disc supports of the valve housing. This modification is not expected to affect the hemodynamics of the valve. The modification is intended to reduce the total surface area of bare metal exposed to the flowing blood, thereby reducing the amount of lethal and sublethal damage caused to blood components, and therefore reducing hemolysis and thromboembolic complications.

The Bjork-Shiley valve consists of a free floating convexo-concave circular disc of pyrolytic carbon suspended in a stellite cage (1). In the valve design in current clinical use, the disc opens to an angle of 56° and is marked by a ring-shaped tantalum radio-opaque marker, allowing visualization of valve function by cinefluoroscopy. In the new modified version, the disc opens to 70° . The Bjork-Shiley valve is at present the most popular heart valve prosthesis, and has been studied critically by our group (1,2).

Size 25, 27 and 29 mm (sewing ring diameter) valves were used in the study. The prosthetic valves were studied under steady flow conditions over a flow rate range of 167 to 500 mL/s in appropriate aortic and mitral valve flow chambers. A six percent-by-weight aqueous Polyol V-10 solution was used as the blood analog fluid at 32°C . The solution is Newtonian with a viscosity of 0.0035 Pa.s and a density of 1015 kg/m^3 . Velocity and shear stress measurements were conducted in the aortic flow channel with the size 27 valves, using a laser-Doppler anemometer system. Pressure drop studies were conducted across all three valve sizes with a Polyol-pentane manometer. Details of the experimental technique and apparatus have been published previously (1,3).

The velocity profiles across the major orifices of all three valve designs show unobstructed flow with high wall shear stresses (see Fig. 1) The velocity profiles measured across the minor orifice of the Bjork-Shiley valve show a region of flow separation near either wall caused by the sewing ring. Two minima exist, caused by the two legs of the bottom strut passing across the minor orifice. The velocity profiles across the minor orifice of both the Hall-Kaster and the modified Hall-Kaster valves also show a region of flow separation near either wall, and a minimum in the center caused by the bottom support extending across the minor orifice (see Fig. 2). Velocity measurements across the Bjork-

Shiley valve indicate a region of stagnation in the immediate downstream vicinity of the tip of the disc, as shown in Fig. 3. The velocity profiles measured below the discs of both Hall-Kaster valve designs indicate only a small region of stagnation downstream of the disc edge. In comparing the velocity profiles of the two Hall-Kaster models, little difference was seen between the two valves. Reducing the size of the metal stops, however, helped reduce the size of the stagnation regions adjacent to these stops. Although little difference was seen between the velocity fields of the two Hall-Kaster designs, the disc of the modified valve was observed to be lifted by approximately 15° from the fully open position, for steady flow rates larger than about 200 mL/s. This effect was probably caused by the turbulent wake region underneath the disc. The phenomenon was noticed with the size 27 aortic and size 29 mitral valves, but was not seen with the size 25 aortic valve, implying that it may be size related. The stagnation region observed in the immediate downstream vicinity of the disc of the new Bjork-Shiley valve is smaller than that observed with the design in current clinical use (2).

All three designs caused elevated wall shear stresses, especially in the major orifice region, which could cause damage to the endothelial lining of the vessel wall adjacent to the valve. The wall shears are, however, lower than those created by the ball and flat disc type valves. Turbulent shear stresses estimated from turbulence intensity measurements indicate turbulent shear stresses on the order of 100 to 200 N/m^2 in the immediate downstream vicinity of all three designs. These turbulent shear stresses are large enough to cause lethal and/or sublethal damage to blood elements, such as red blood cells and platelets. The regions of flow stagnation and flow separation observed adjacent to the superstructures of all three valves, could lead to thrombus formation and/or excess tissue overgrowth on and around the valve prostheses (1).

The pressure drop studies (see Fig. 4) with all three valve sizes, indicate little significant difference between the two Hall-Kaster models, while the new Bjork-Shiley valves showed a 20% to 30% improvement compared to the current clinical model Bjork-Shiley valves.

Acknowledgements

This work was supported by the Georgia Heart Association. The prosthetic valves were provided by Kastec Inc., St. Paul, MN., and Shiley Laboratories Inc., Irvine, CA.

References

1. Yoganathan, A. P., Corcoran, W. H., Harrison, E. C., and Carl, J. R., "The Bjork-Shiley Aortic Prosthesis: Flow Characteristics, Thrombus Formation and Tissue Overgrowth," Circulation, Vol. 53, 1978, pp. 70-76.
2. Yoganathan, A. P., Reamer, H. H., Corcoran, W. H., and Harrison, E. C., "The Bjork-Shiley Aortic Prosthesis: Flow Characteristics of the Present Model Vs the Convexo-Concave Model," Scandinavian Journal of Thoracic and Cardiovascular Surgery, Vol. 14, 1980, pp. 1-5.
3. Yoganathan, A. P., Reamer, H. H., Corcoran, W. H., and Harrison, E. C., "A Laser-Doppler Anemometer to Study Velocity Fields in the Vicinity of Prosthetic Heart Valves," Medical and Biological Engineering and Computing, Vol. 17, 1979, pp. 38-44.